Observation of oscillation symmetry in nuclei excited state masses and widths

B. Tatischeff*
Universté Paris-Saclay, CNRS/IN2P3, IJCLab, Orsay Cedex, France

A systematic study of hadron masses and widths shows regular oscillations which can be fitted by a simple cosine function. This oscillation symmetry is observed studing the differences between adjacent masses of each nucleon family plotted versus the corresponding mean masses. It is also observed in the widths of excited levels, when plotted versus the corresponding masses.

We observe the same distribution of periods versus the atomic number A, between the nuclear mass data and the periods describing the atomic energy levels of several neutral atoms.

The nuclear level widths data are analysed in a way similar to that done for the masses.

The distributions of the mass data between some different body families are compared.

PACS numbers: 21.10.-k, 21.10.Dr, 21.10.Tg, 21.80.+a, 27.00.00

I. INTRODUCTION

The properties of several composite objects bound by several forces acting on their masses, have been discussed recently. These objects are bound by at least one attractive and one repulsive interaction. Otherwise the composite masses will either disintegrate, or mix into a totally new object, like plasma for example, with loss of the individual components. In consequence of these opposite forces, similarly to classical physics, the mass sequence of these objects could show an oscillating behaviour. Such existing behaviours have been indeed observed in masses of fundamental particles [1] and nuclei [2]. Their masses are described by Schrödinger equations containing opposite kinetic and potential interactions. Although such symmetry property is not justified for the corresponding widths, an attempt to observe similar oscillations has been also studied.

Similar studies have also be done for the opposite side of body masses, namely the very large masses, that is to say in astrophysics [3] [4]. Here the bodies are submitted to opposite gravitational forces and centrifugal forces related to their kinetic energies.

In nuclear scope, the properties of the electromagnetic transition masses and widths between several nuclei excited state levels have been studied [2].

The present paper is devoted to a similar study applied to the masses and widths of the excited states of many nuclei.

The differences between adjacent masses versus their corresponding mean masses are studied. The figures show the mass variations through the distribution:

$$m_{(n+1)} - m_n = f[(m_{(n+1)} + m_n)/2] \qquad (1)$$

where $m_{(n+1)}$ corresponds to the (n+1) mass value. The function displays the successive mass differences, plotted versus the mean mass value of both masses (n) and (n+1). The values obtained using equation (1) will be named "data" below. The fits are obtained using a cosine function:

$$\Delta M = \alpha(1 + cos((M - M_0)/M_1)) * exp(\beta.M) \qquad (2)$$

Depending on the figures and tables, the units are either MeV, or mass number A. The parameter values are given in tables presented below. The oscillation periods are P $= 2\ \pi M_1$. The study of the amplitude of oscillations deserves theoretical studies which are outside the scope of the present work. The start of the fit is arbitrary involving the vanishing of M_0. The fits are therefore done with three adjustable parameters: α, M_1, and β.

Whereas smaller periods than those given are also solution of the fit, we keep the largest possible one.

These distributions do not create oscillations when these do not exist in data. Moreover it is obvious that random sets of "data" cannot be fitted by regular oscillating distributions.

The energy levels of many nuclei, are studied through the distribution (1), and fitted with the cosine function (2). The corresponding oscillation periods are named: "P". The nuclei of the considered mass range 4≤A≤194, are gathered through reduced mass ranges. The period variation inside each range is studied. It appears that, when plotted versus the nuclei masses, the periods exhibit also an oscillating behaviour. The correspoding periods are called: "PP". Finally, the PP periods of the different nuclei ranges, exhibit again an oscillating behaviour which period is named "PPP".

The nuclei level widths are also read and their data analysed in a way similar to that done for the masses. A dedicated discussion concerns the nuclei level widths.

* tati@ipno.in2p3.fr

II. APPLICATION TO NUCLEI LEVEL MASSES

When not specified, the excited state masses of most nuclei studied below, are read using [5].

A. Study of doubly magic nuclei

The shell model explains the doubly magic nuclei properties, since they correspond to filled shells. These properties are: larger binding energy per nucleon and hence larger stablility, but also larger excited state spacings. Fig. 1 shows in inserts (a), (b), (c), (d), and (e) respectively, the "data" for ^{4}He [6] (which oscillating period P=2.07 MeV), ^{16}O [7]-[8] (P=4.6 MeV), ^{40}Ca (P=2.23 MeV), ^{48}Ti (P=1.32 MeV), and ^{208}Pb [9] (P=2.07 MeV). We observe wavy shapes for all five nuclei, and increasing absorption for the oscillations in increasing mass nuclei. The corresponding quantitative information is shown in Table (I). Beyond the first "data", the fits no more agree with "data", implying the need for additionnal assumptions. This is observed, all the more the nuclei mass increases. The fit inside the lowest mass distribution, fig.1(a), which corresponds to ^{4}He nucleus, describe completely the "data". The poor

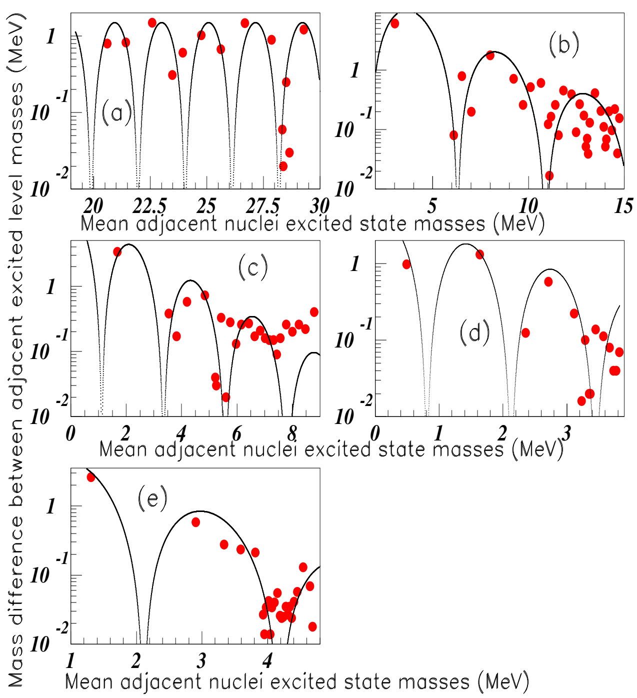

FIG. 1. Color on line. Mass difference between successive masses, plotted versus the corresponding mean masses of the main double-magic nuclei. Inserts (a), (b), (c), (d), and (e), show the data respectively for ^{4}He, ^{16}O, ^{40}Ca, ^{48}Ti, and ^{208}Pb. (See text.)

knowledge of the ^{48}Ca level masses prevents to study this nuclei. ^{48}Ti being not a double-magic nucleus, the corresponding period is smaller than the others shown in table I. Fig. 2 shows the variation of the periods for

TABLE I. Quantitative information concerning the oscillation behaviour of the doubly magic nuclei shown in fig. 1

nuclei	fig.	α	β	P(MeV)
^{4}He	1(a)	0.75	0	2.07
^{16}O	1(b)	19	-0.35	4.6
^{40}Ca	1(c)	7.5	-0.57	2.23
^{48}Ti	1(d)	2.1	-0.58	1.32
^{208}Pb	1(e)	5	-0.81	2.07

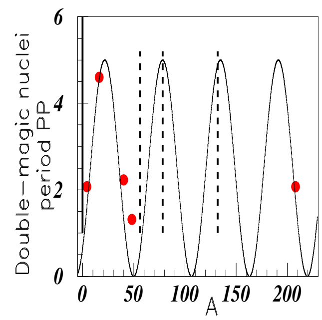

FIG. 2. Color on line. Variation of periods fitting the excited state masses of doubly magic nuclei (See text.)

doubly magic nuclei plotted versus the mass number A. This variation is well fitted with PP=56.5 mass number A. Vertical dashed lines correspond to other doubly magic nuclei, namely to A=56, 78, and A=132. The fits predict rather large periods, P≈5 for A=78 and 132 . This is not observed in other nuclei since the levels of ^{78}Ni, or ^{100}Sn, are not known. The level sequence of ^{132}Sn does not show a behaviour which agrees with such period. The fit predicts P≈1.3 for ^{56}Ni , i.e. a value close to the one obtained for ^{48}Ti.

The oscillating mass periods for a large number of nuclei studied, are given below. The mass parameters of the fits for nuclei with A larger than ^{48}Ti will be shown later on in Table VIII. They will be compared with corresponding parameters extracted from the widths Γ which will be discussed after the masses in forthcoming tables and figures.

B. Study of A≤21 nuclei

The mass differences between successive masses, plotted versus the same mean masses for several A≤21 nuclei are plotted in figs. 3, 4, 5, and 6.

Fig. 3 shows the mass difference between successive masses, plotted versus the corresponding mean masses for ^{7}Li, ^{8}Li, ^{9}Be, and ^{10}B [10] [11] in inserts (a), (b), (c), and (d) respectively. The cosine function describes well

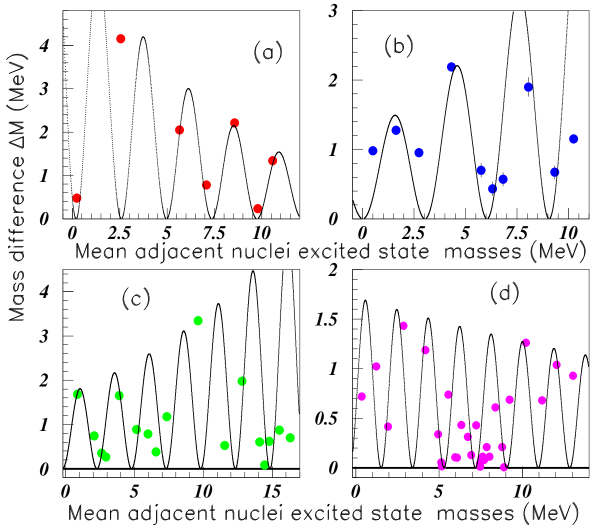

FIG. 3. Color on line. Mass difference between successive masses, plotted versus the corresponding mean masses of four nuclei. Inserts (a), (b), (c), and (d) show successively the "data" for ^{7}Li, ^{8}Li, ^{9}Be, and ^{10}B. (See text.)

the experimental oscillations for the ^{7}Li, ^{8}Li, and ^{9}Be nuclei, and at least the first "data" of ^{10}B nuclei. The distribution does not fit the ^{10}B "data" for excitation energies between 6 and 8 MeV.

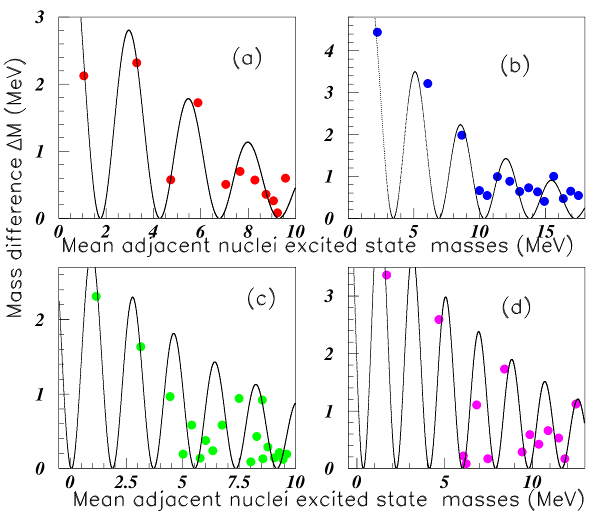

FIG. 4. Color on line. Mass difference between successive masses, plotted versus the corresponding mean masses of four nuclei. Inserts (a), (b), (c), and (d) show successively the "data" for ^{11}B, ^{12}C, ^{14}N, and ^{10}Be. (See text.)

Fig. 4 shows the "data" for ^{11}B, ^{12}C, ^{14}N, and ^{10}Be nuclei [12] in inserts (a), (b), (c), and (d) respectively.

Fig. 5 shows the "data" for ^{13}N, ^{15}N, ^{18}Ne, and ^{21}Ne nuclei [13] [5] [14] in inserts (a), (b), (c), and (d) respectively.

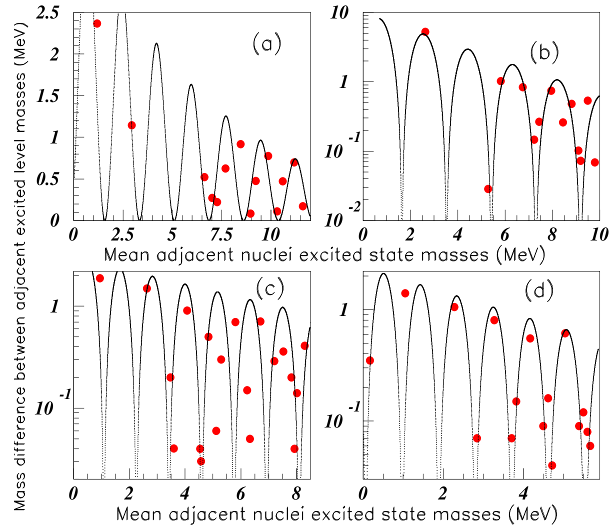

FIG. 5. Color on line. Mass difference between successive masses, plotted versus the corresponding mean masses of four nuclei levels. Inserts (a), (b), (c), and (d) show successively the "data" for ^{13}N, ^{15}N, ^{18}Ne, and ^{21}Ne. (See text.)

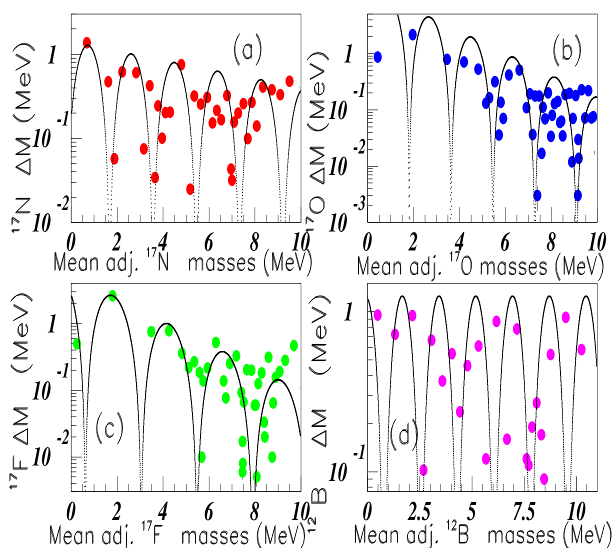

FIG. 6. Color on line. Mass difference between successive masses, plotted versus the corresponding mean masses of four nuclei levels. Inserts (a), (b), (c), and (d) show successively the "data" for ^{17}N, ^{17}O, ^{17}F, and ^{12}B. (See text.)

The "data" in all four inserts are well fitted by the cosine function. The oscillatory behavior is particularly well obtained in inserts (a), (b), and (d) which corresponds to ^{21}Ne nucleus.

Fig. 6 shows the data for ^{17}N, ^{17}O, ^{17}F [15], and ^{12}B nuclei in inserts (a), (b), (c), and (d) respectively. The fits get spoiled for excitation energies larger than 5 MeV.

C. Study of ^{23}Mg≤A≤^{33}Cl nuclei

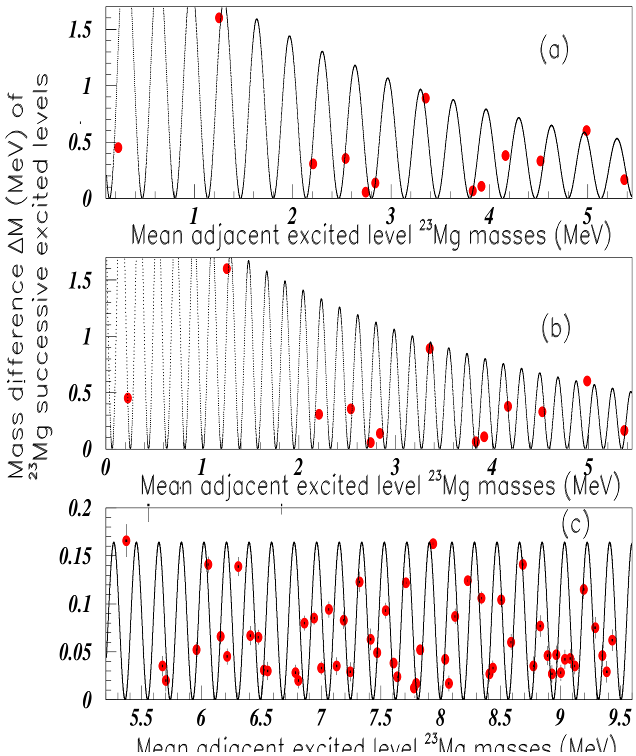

FIG. 7. Color on line. Mass difference between successive masses, plotted versus the same mean masses of ^{23}Mg. (See text.)

Fig. 7 shows the "data" and fit for ^{23}Mg nucleus [16]. We observe again an oscillatory behaviour but also a reduction of periods for increasing masses. These "data", thanks to the large number of known excited state levels, allow to discuss the given precision. The period obtained is P = 0.333 MeV for "data" lower than 5.4 MeV excitation energy (insert(a)). For larger A the number of "data" increases, involving a smaller period P=0.188 MeV shown in insert (c). However the same period P=0.188 MeV, as displayed in insert (c), fits the "data" lower than 5.4 MeV. This is shown in insert (b). In all figures, the extracted periods are as the largest possible. It is clear that periods, smaller than those given, may be also possible.

Fig. 8 shows the "data" for ^{26}Mg in insert (a) P = 1.38 MeV, ^{27}Al in insert (b) P = 1.07 MeV, ^{28}Si [17] in insert (c) P = 1.26 MeV, and ^{29}Si in insert (d) P = 0.80 MeV. The oscillatory behaviour is clearly present for the first 8-10 masses. The agreement between "data" and fit spoils for larger "data", specially for ^{26}Mg and ^{28}S.

Fig. 9 shows the "data" for ^{24}Mg in insert (a) P = 1.005 MeV, ^{25}Mg in insert (b) P = 0.503 MeV, ^{30}P in insert (c) P = 0.628 MeV, and ^{33}Cl (red data) and ^{33}S (blue data) in insert (d) P = 0.942 MeV.

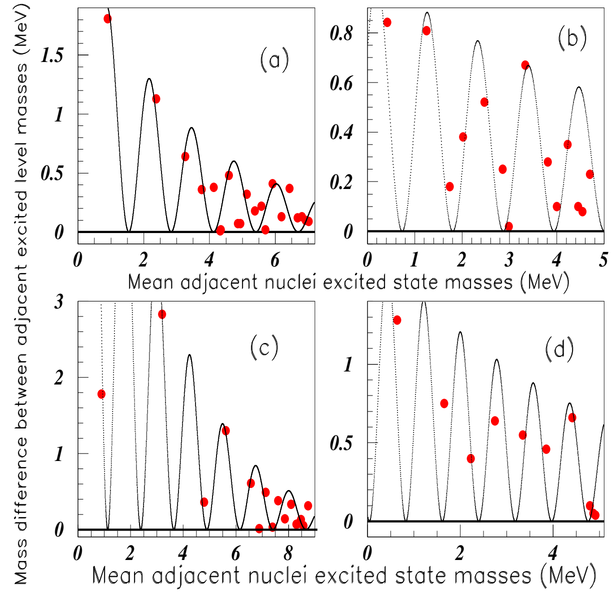

FIG. 8. Color on line. Mass difference between successive masses, plotted versus the same mean masses of ^{26}Mg in insert (a), ^{27}Al in insert (b), ^{28}Si in insert (c), and ^{33}Cl in insert (d). (See text.)

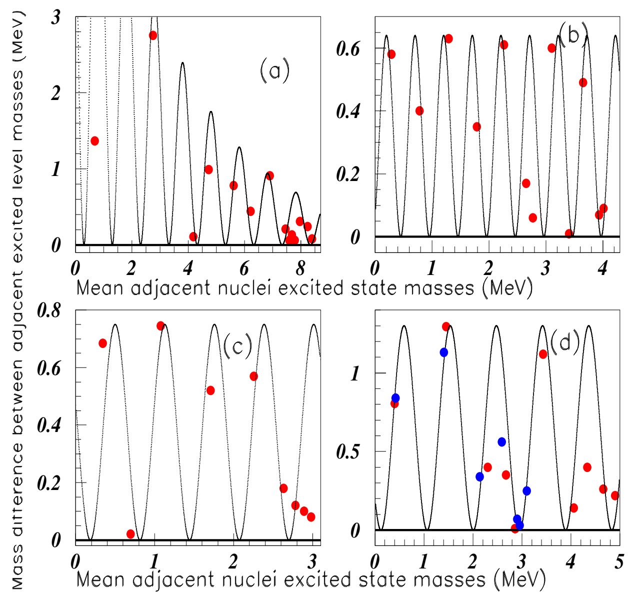

FIG. 9. Color on line. Mass difference between successive masses, plotted versus the same mean masses of ^{24}Mg in insert (a), ^{25}Mg in insert (b), ^{30}P in insert (c), and ^{33}S and ^{33}Cl in insert (d). (See text.)

Fig. 10 shows the variation, versus A, of the oscillating periods fitting the excited state masses of ^{4}He≤A≤^{33}Cl nuclei. The distribution PP=3.20 A oscillates and at the same time decreases with increasing masses.

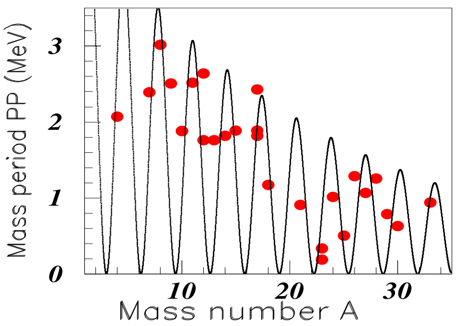

FIG. 10. Color on line. The figure shows the variation, versus A, of the periods fitting the excited state masses of ^{4}He≤A≤^{33}Cl nuclei. (See text.)

TABLE II. Quantitative information concerning the oscillation behaviour of some nuclei in the mass range 61≤A≤74, shown in fig. 12.

name	fig.	α	β	P(MeV)
$^{61}_{29}$Cu	11(a)	0.34	-0.59	0.44
$^{64}_{30}$Zn	11(b)	1.2	-0.85	0.817
$^{65}_{29}$Cu	11(c)	0.72	-0.67	0.69
$^{66}_{30}$Zn	11(d)	1.1	-0.67	0.82
$^{70}_{32}$Ge	11(e)	1.31	-0.79	0.68
$^{74}_{32}$Ge	11(f)	0.5	-0.33	0.377

D. Study of ^{61}Cu≤A≤^{74}Ge nuclei

Fig. 11 shows the mass difference between successive masses, plotted versus the same mean masses of several nuclei [18]: $^{61}_{29}$Cu (in red) in insert (a); $^{64}_{30}$Zn (in blue) in insert (b); $^{65}_{29}$Cu (in red) in insert (c); $^{66}_{30}$Zn (in red) in insert (d); $^{70}_{32}$Ge (in blue) in insert (e); and $^{74}_{32}$Ge (in red) in insert (f). Two levels are missing in the $^{74}_{32}$Ge table of [18]. One level, present in other papers is introduced in fig. 11.

Table II gives the quantitative information.

Fig. 12 shows these periods versus A fitted with the period PP=2.51 A.

E. Study of ^{90}Zr≤A≤^{94}Mo nuclei

Fig. 13 shows the "data" [5] and fits of $^{90}_{40}$Zr (in red) and $^{90}_{38}$Sr (in blue) in insert (a); $^{90}_{37}$Rb (in red) and $^{90}_{41}$Nb (in blue) in insert (b); $^{91}_{39}$Y (in red), $^{91}_{40}$Zr (in blue), and $^{91}_{41}$Nb (in green) in insert (c); $^{92}_{40}$Zr (in red) and $^{92}_{42}$Mo (in green) in insert (d); $^{93}_{40}$Zr (in red) and $^{93}_{42}$Mo (in blue) in insert (e); and $^{94}_{40}$Zr (in red) and $^{94}_{42}$Mo (in blue) in insert (f).

All data exhibit oscillating behaviours. Table III shows the corresponding periods. The eighth mass of $^{90}_{41}$Nb

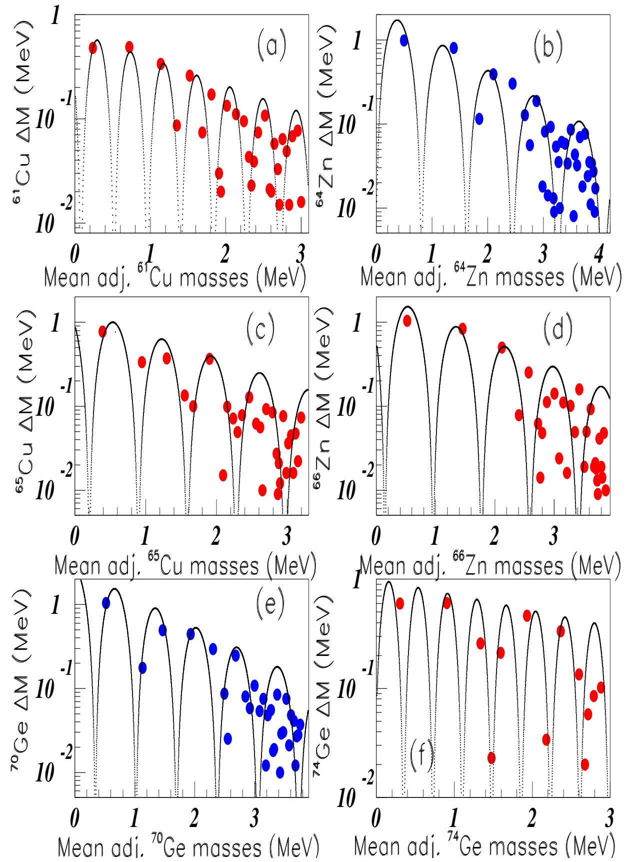

FIG. 11. Color on line. Mass difference between successive masses, plotted versus the same mean masses of several nuclei: $^{61}_{29}$Cu (red) in insert (a); $^{64}_{30}$Zn (blue) in insert (b); $^{65}_{29}$Cu (red) in insert (c); $^{66}_{30}$Zn (red) in insert (d); $^{70}_{32}$Ge (blue) in insert (e); and $^{74}_{32}$Ge (red) in insert (f). (See text and Table II.)

(fig. 13(b)) is given to be either 0.825 MeV, or 1.321 MeV in [5]. The intermediate value between both is used without any effect for the distribution. The "data" for some nuclei are scarce. The major result from fig. 13 lies in the observation that although the excited level masses vary from one nuclei to another, they take place in the same distribution, for same A nuclei. Although their masses are different, shown by red, blue, and green data, however they take place in a common fit, with the same period.

Fig.14 shows the period of oscillation PP for 90≤A≤94 nuclei (see fig. 13). The periods for even-even nuclei are shown with full red circles. The period for odd-odd nucleus is shown with a full blue square. The periods for even-odd nuclei are shown with full magenta up-side triangles. The pairing effect is clearly observed in the oscillating periods of excited level masses in these nuclei. Indeed the periods corresponding to even-even nuclei are larger than the periods for odd-odd or odd-even nuclei.

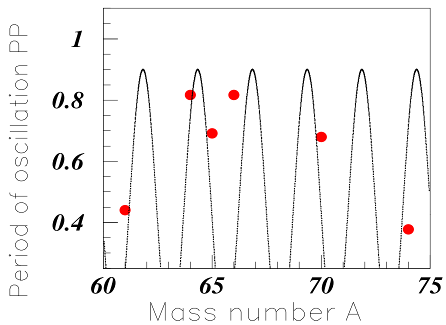

FIG. 12. Color on line. Variation of the mass oscillating periods observed for nuclei from ^{61}Cu to ^{74}Ge, plotted versus the mass number A. (See text.)

TABLE III. Quantitative information concerning the oscillation behaviour of the nuclei shown in figure 14.

name	fig.color	α	β	P(MeV)
$^{90}_{40}$Zr	13(a)red	1.04	-0.23	0.942
$^{90}_{38}$Sr	13(a)blue	1.04	-0.23	0.942
$^{90}_{37}$Rb	13(b)red	0.7	-0.18	0.704
$^{90}_{41}$Nb	13(b)blue	0.7	-0.18	0.704
$^{91}_{39}$Y	13(c)red	0.64	-0.49	0.653
$^{91}_{40}$Zr	13(c)blue	0.64	-0.49	0.653
$^{91}_{41}$Nb	13(c)green	0.64	-0.49	0.653
$^{92}_{40}$Zr	13(d)red	4.2	-1.22	0.817
$^{92}_{42}$Mo	13(d)green	4.2	-1.22	0.817
$^{93}_{40}$Zr	13(e)red	0.57	-0.39	0.653
$^{93}_{42}$Mo	13(e)blue	0.57	-0.39	0.653
$^{94}_{40}$Zr	13(f)red	0.49	0	0.735
$^{94}_{42}$Mo	13(f)blue	0.49	0	0.735

F. Study of some Palladium isotopes

The distributions of excited masses of palladium isotopes [5] 103≤Pd≤110 are shown in fig. 15. Insert (a) shows the "data" and fit for ^{103}Pd (red on line) and ^{104}Pd (blue on line) fitted with a period P = 0.18 MeV. Insert (b) shows the "data" and fit for ^{105}Pd (red on line) with a period P = 0.18 MeV. Insert (c) shows the "data" and fit for ^{106}Pd (blue on line) with a period P = 0.283 MeV. Insert (d) shows the "data" and fit for ^{107}Pd (red on line) with a period P = 0.283 MeV. Insert (e) shows the "data" and fit for ^{108}Pd (blue on line) with a period P = 0.653 MeV. Finally insert (f) shows the "data" and fit for ^{109}Pd (red on line) with a period P = 0.327 MeV.

Fig. 16 and Table IV show the period PP of the Pd isotopes fitted with PP = 2.07 A. The maximum value (PP = 0.65 A) for ^{108}Pd, reflects the neutron magic number (N=82) of this isotope, the periods slowly decreasing at both sides of this isotope when the neutron number moves off from 82.

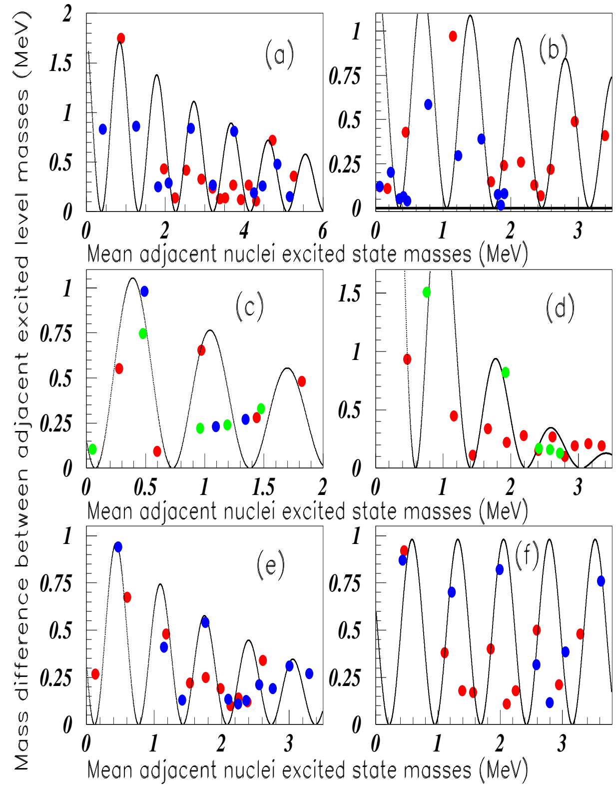

FIG. 13. Color on line. Mass difference between successive masses, plotted versus the same mean masses of several isotopes: $^{90}_{40}$Zr (red) and $^{90}_{38}$Sr (blue) in insert (a); $^{90}_{37}$Rb (red) and $^{90}_{41}$Nb (blue) in insert (b); $^{91}_{39}$Y (red), $^{91}_{40}$Zr (blue), and $^{91}_{41}$Nb (green) in insert (c); $^{92}_{40}$Zr (red) and $^{92}_{42}$Mo (green) in insert (d); $^{93}_{40}$Zr (red) and $^{93}_{42}$Mo (blue) in insert (e); and $^{94}_{40}$Zr (red) and $^{94}_{42}$Mo (blue) in insert (f). The data are plotted versus the mean adjacent nuclei excited state masses (in MeV). (See text and Table IV.)

G. Study of some Cerium isotopes

The excited masses [5] of some cerium isotopes, using the distributions (1) and fit (2) are shown in fig. 17. The fitted periods are given in Table V.

Fig. 17(a) shows the "data" and fit for ^{138}Ce (red on line) with a period P = 1.445 MeV. Fig. 17(b) shows the "data" and fit for ^{140}Pd (blue on line) with a period P = 1.037 MeV. Fig. 17(c) shows the "data" and fit for ^{141}Pd (blue on line) with a period P = 0.515 MeV. Fig. 17(d) shows the data and fit for ^{142}Pd (red on line) with a period P = 0.503 MeV.

The variation of the oscillating periods PP of Ce isotpes, is shown with full circles and PP=7.79 A in fig. 19 (blue on line).

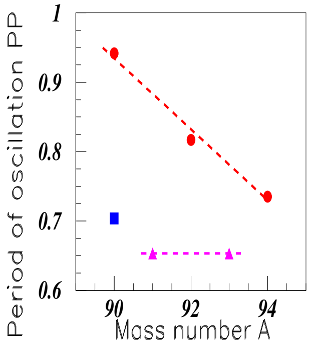

FIG. 14. Color on line. Periods of the mass oscillation of nuclei with mass number 90≤ A ≤94 listen in table IV. The periods of even-even, even-odd, and odd-odd nuclei are shown respectively by full red circles, full magenta up-side triangles, and full blue square. (See text.)

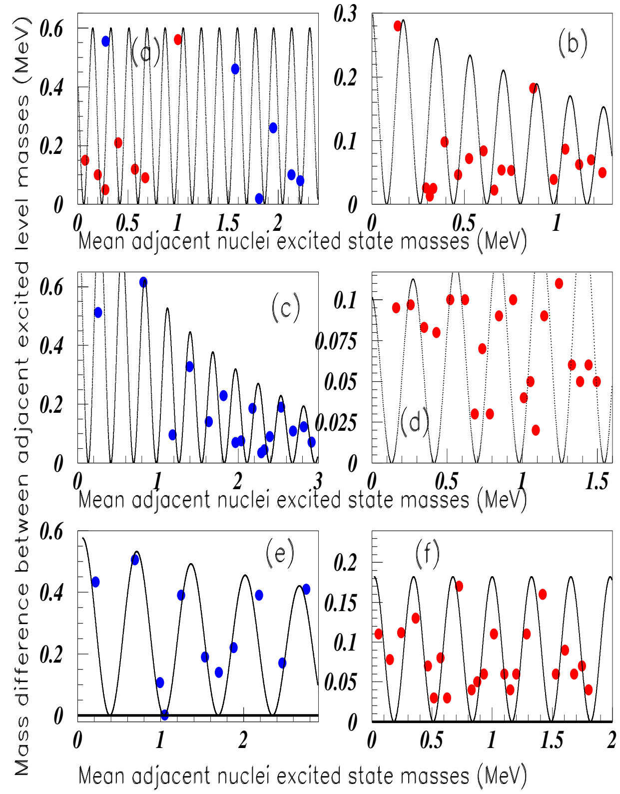

FIG. 15. Color on line. Mass difference between successive masses, plotted versus the same mean masses of Pd isotopes. Inserts (a) to (f), correspond to isobars 103 to 110 with data from two isobars in insert (a). (See text and Table IV.)

TABLE IV. Quantitative information concerning the oscillation behaviour of the palladium nuclei shown in fig. 16.

nuclei	fig.	α	β	P(MeV)
$^{103}_{46}$Pd	15(a)red	0.30	9	0.18
$^{104}_{46}$Pd	15(a)blue	0.30	0	0.18
$^{105}_{46}$Pd	15(b)red	0.16	-0.59	0.18
$^{106}_{46}$Pd	15(c)red	0.51	-0.59	0.283
$^{107}_{46}$Pd	15(d)red	0.052	0.29	0.283
$^{108}_{46}$Pd	15(e)blue	0.29	-0.12	0.653
$^{109}_{46}$Pd	15(f)red	0.091	0	0.327

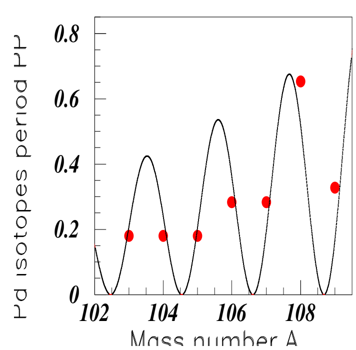

FIG. 16. Color on line. Variation of the mass periods fitting the excited state masses of palladium isotopes (See text.)

H. Study of some Samarium isotopes

The excited masses [5] of several isotopes of Samarium, using the distribution (1) and fit (2), are shown in fig. 18. Insert (a) shows the "data" for isotope 145 (red on line), insert (b) shows the "data" for isotope 147 (blue on line), insert (c) shows the "data" for isotope 148 (blue on line), insert (d) shows the "data" for isotope 149 (red on line), insert (e) shows the "data" for isotope 150 (red on line), insert (f) shows the "data" for isotope 151 (blue on line), insert (g) shows the "data" for isotope 152 (blue on line), and insert (h) shows the "data" for isotope 154 (red on line). The fitted periods are given in table V. The variation of fitted periods from Ce isotopes (blue) and Sm isotopes (full red squares) are shown in fig. 19. These data exhibit again an oscillatory shape with the period PP = 7.79 mass number A.

I. Study of several nuclei in the range $^{186}_{76}$Os≤A≤$^{192}_{79}$Au

Fig. 20 shows the "data" and fit of nuclei in the range 186 ≤ A ≤ 192. Insert (a) shows "data" and fit of ^{186}Os, insert (b) shows "data" and fit of ^{187}Os in red and ^{187}Re in blue, insert (c) shows "data" and fit of ^{188}Os in red and ^{188}Ir in green, insert (d) shows "data" and fit of ^{189}Os in red and ^{189}Ir in green, insert (e) shows "data" and fit of ^{190}Os in red and ^{190}Pt in blue, and insert (f) shows "data" and fit of ^{192}Os in red, ^{192}Pt in blue, and ^{192}Au in green.

The "data" of all inserts in fig. 20 corresponds to the same mass number "A". Some "data" scatter more than

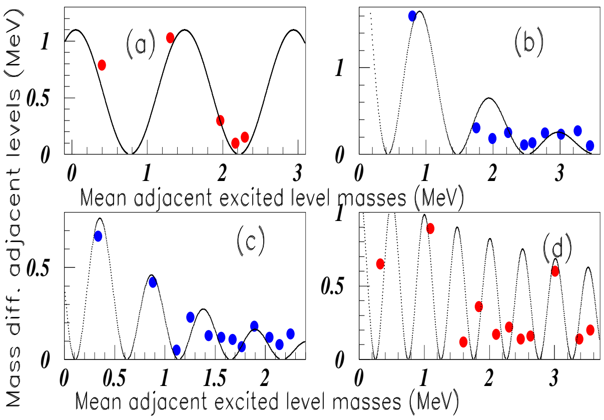

FIG. 17. Color on line. Mass difference between successive masses, plotted versus the same mean masses of Ce isotopes. Inserts (a) to (d), correspond to A=138, 140, 141, and 142 isotopes. (See text and Table VI.)

TABLE V. Quantitative information concerning the oscillation behaviour of nuclei with mass A≈150 shown in figs. 18 and 19.

nuclei	fig.	α	β	P(MeV)
$^{138}_{58}$Ce	17(a)red	0.55	0	1.445
$^{140}_{58}$Ce	17(b)blue	1.9	-0.9	1.037
$^{141}_{58}$Ce	17(c)blue	0.55	-1.0	0.515
$^{142}_{58}$Ce	17(d)red	0.59	-0.18	0.503
$^{145}_{62}$Sm	18(a)red	0.82	-1.13	0.754
$^{147}_{62}$Sm	18(b)blue	0.54	-1.8	0.754
$^{148}_{62}$Sm	18(c)blue	0.85	-1.20	0.471
$^{149}_{62}$Sm	18(d)red	0.147	-0.91	0.333
$^{150}_{62}$Sm	18(e)red	0.38	-0.932	0.188
$^{151}_{62}$Sm	18(f)blue	0.065	0	0.126
$^{152}_{62}$Sm	18(g)blue	0.29	0.15	0.503
$^{154}_{62}$Sm	18(h)red	0.23	0	0.503

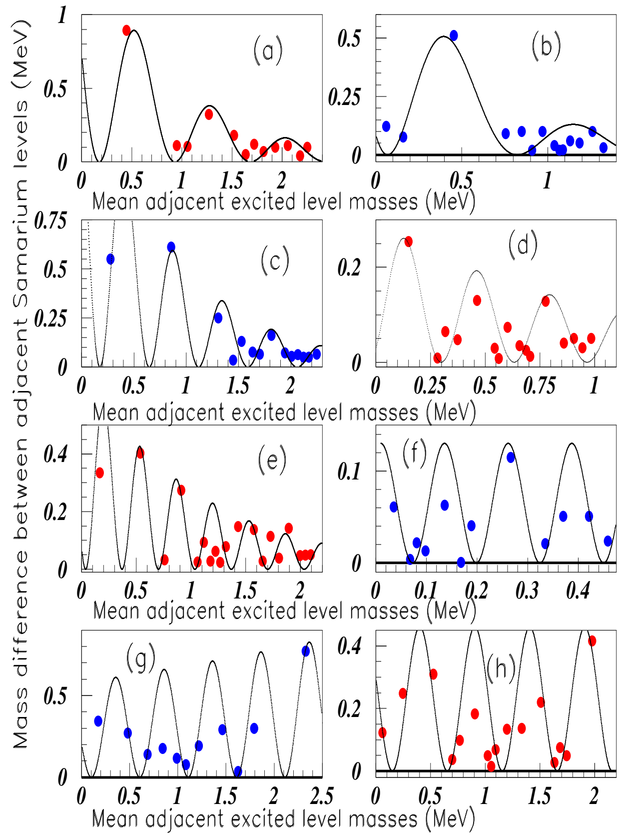

FIG. 18. Color on line. Mass difference between successive masses, plotted versus the same mean masses of Sm isotopes. Inserts (a) to (h), correspond to mass numbers 145 to 154. (See text and Table VI.)

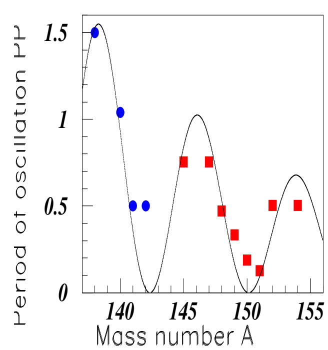

FIG. 19. Color on line. Oscillation periods of the excited level masses of Ce isotopes (in blue), and Sm isotopes (in red). (See text.)

in previous figures. However the "data" of ^{189}Ir, ^{190}Pt, and ^{192}Pt are well fitted. They are all three nuclei with an even number of neutrons. The ^{188}Ir nucleus is badly known. Indeed the number of "data" is small (green points in insert (c)). The oscillating periods of excited level masses of nuclei studied in fig. 20, are given in table VI.

Fig. 21 shows the variation of the mass periods corresponding to $^{186}_{76}$Os$\leq$A$\leq^{192}_{79}$Au nuclei. These "data" are fitted with an oscillating behaviour obtained with a period = 3.016 A.

III. APPLICATION TO NUCLEI LEVEL WIDTHS

The oscillatory behaviour of masses was expected, as said in the introduction, being the consequence of opposite interactions in the Schrödinger equation, and more generally in all composite objects. No equivalent prop-

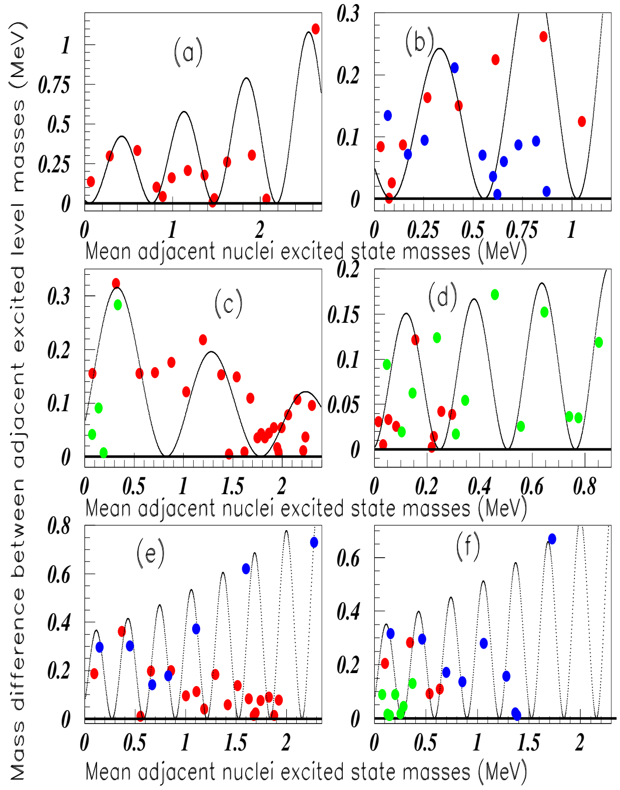

FIG. 20. Color on line. Mass difference between successive masses, plotted versus the same mean masses of nuclei in the range $186 \leq A \leq 192$. Insert (a) shows "data" and fit of ^{186}Os, insert (b) shows "data" and fit of ^{187}Os in red and ^{187}Re in blue, insert (c) shows "data" and fit of ^{188}Os in red and ^{188}Ir in green, insert (d) shows "data" and fit of ^{189}Os in red and ^{189}Ir in green, insert (e) shows "data" and fit of ^{190}Os in red and ^{190}Pt in blue, and insert (f) shows "data" and fit of ^{192}Os in red, ^{192}Pt in blue, and ^{192}Au in green. (See text and Table VII.)

TABLE VI. Quantitative information concerning the mass oscillation behaviour of the nuclei shown in fig. 20

name	fig.	α	β	P(MeV)
$^{186}_{76}$Os	20(a)red	0.193	0.45	0.691
$^{187}_{76}$Os	20(b)red	0.087	0.50	0.572
$^{187}_{75}$Re	20(b)blue	0.087	0.50	0.572
$^{188}_{76}$Os	20(c)red	0.191	-0.49	0.955
$^{188}_{77}$Ir	20(c)green	0.191	-0.49	0.955
$^{189}_{76}$Os	20(d)red	0.093	0	0.192
$^{189}_{77}$Ir	20(d)green	0.093	0	0.192
$^{190}_{76}$Os	20(e)red	0.160	0.40	0.302
$^{190}_{78}$Pt	20(e)blue	0.160	0.40	0.302
$^{192}_{76}$Os	20(f)red	0.160	0.44	0.314
$^{192}_{78}$Pt	20(f)blue	0.160	0.44	0.314
$^{192}_{79}$Au	20(f)green	0.160	0.44	0.314

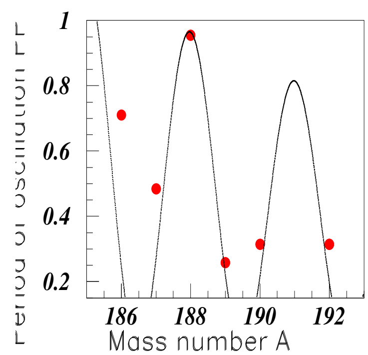

FIG. 21. Color on line. Variation of the mass periods corresponding to $^{186}_{76}$Os$\leq$A$\leq^{192}_{79}$Au nuclei. (See text)

erty exists for the level widths. The study of possible oscillations in the level widths, is however considered below. The widths Γ are in kev and the masses in MeV. The figs. show the widths versus the corresponding masses.

Fig. 22 shows the oscillating behaviour of the total widths of ^{11}B, ^{12}C, ^{14}N, and ^{10}Be in inserts (a), (b), (c), and (d) respectively. The important extention of these values involve the use of log scale. Nice fits are observed. The corresponding periods are given in table IX.

Fig. 23 shows the oscillating behaviour of the total widths of ^{8}Be, ^{13}N, ^{13}C, and ^{15}O in inserts (a), (b), (c), and (d) respectively.

Fig. 24 shows the oscillating behaviour of the total widths of ^{8}Li, ^{9}Be, ^{16}N, and ^{16}O in inserts (a), (b), (c), and (d) respectively. The fit between data and cosine function is very good for ^{8}Li insert (a), and ^{9}Be insert (b).

Fig. 25 shows the oscillating behaviour of the total widths of ^{7}Li, ^{10}B, ^{15}N, and ^{17}O in inserts (a), (b), (c), and (d) respectively.

Fig. 26 shows the oscillating behaviour of the total widths of ^{18}F and ^{18}O, plotted versus the corresponding masses, and fits in inserts (a) and (b). Both nuclei have the same A, but are odd-odd first, then even-even. Their level widths are different, however their data are fitted with the same period P = 0.145 MeV.

We observe that the five previous figures figs. 22-26, showing the nuclei level widths are nicely fitted with our simple cosine function. The corresponding periods are given in table VII.

Fig. 27 shows the variation, of the previous periods again fitted with a cosine function. The mass period (insert (a)) is PP=19.16 A, the width period (insert (b)) is PP=2.042 A. The fit of the widths agree well with data.

Fig. 28 shows the variation of the ratio of width versus mass periods fitted with P = 3.267 A. The general oscillation shape is reproduced since the fit describes rather correctly the data.

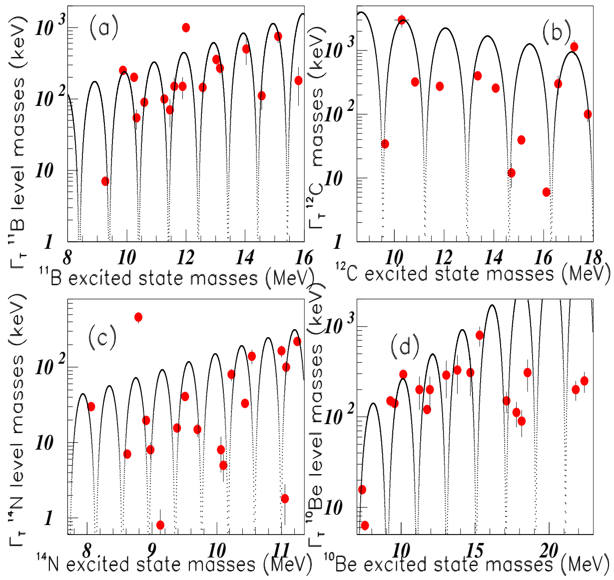

FIG. 22. Color on line. Variation of some nuclei widths. Inserts (a), (b), (c), and (d) show respectively the data and fit of ^{11}B, ^{12}C, ^{14}N, and ^{10}Be. (See text).

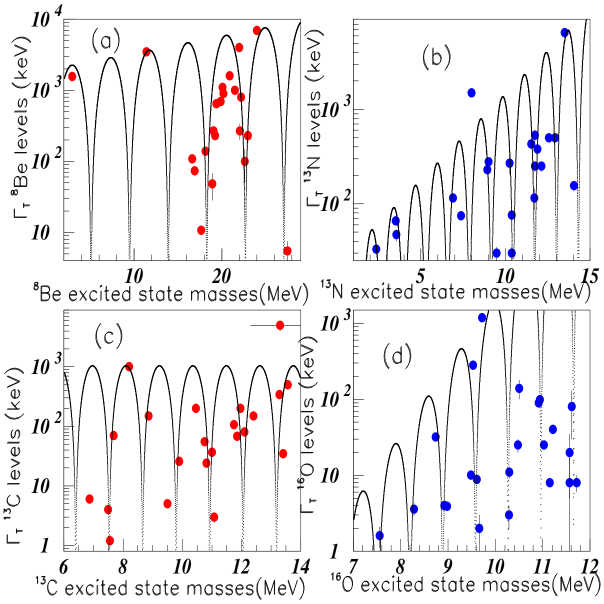

FIG. 23. Color on line. Variation of some nuclei widths. Inserts (a), (b), (c), and (d) show respectively the data and fit of ^{8}Be, ^{13}N, ^{13}C, and ^{15}O. (See text).

IV. DISCUSSION

A large number of excited state level masses of unflavoured nuclei, have been studied for many nuclei, using the distribution (1). All data, restricted to the first ≈10 lower masses, have been fitted by a cosine function (2) giving rise to oscillating periods P. Indeed, above the first ≈ 10^{th} excited levels, the number of states increases

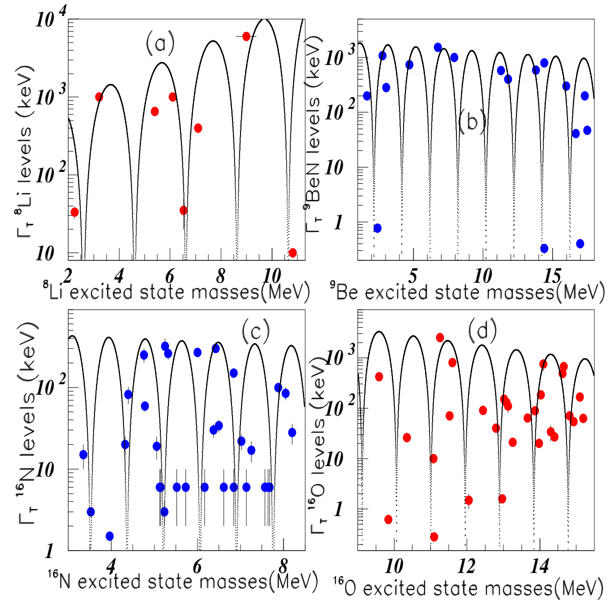

FIG. 24. Color on line. Variation of some nuclei widths. Inserts (a), (b), (c), and (d) show respectively the data and fit of ^{8}Li, ^{9}Be, ^{16}N, and ^{16}O. (See text).

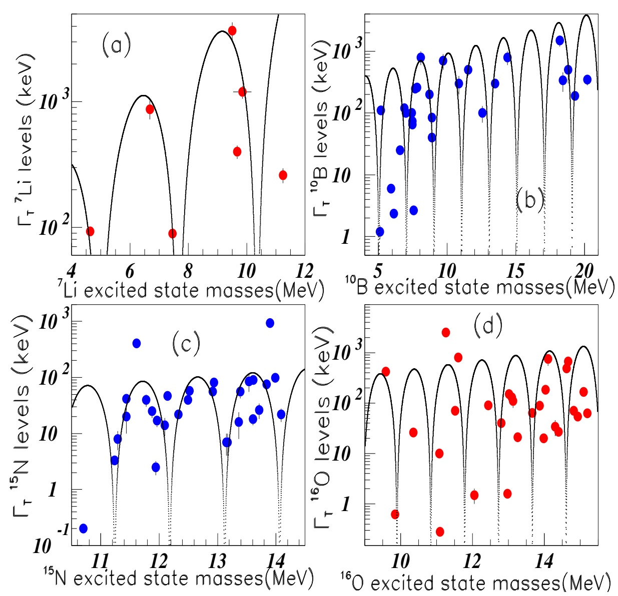

FIG. 25. Color on line. Variation of some nuclei widths. Inserts (a), (b), (c), and (d) show respectively the data and fit of ^{7}Li, ^{10}B, ^{15}N, and ^{17}O. (See text).

fast, and the previous simple oscillations are sometimes no more observed. Therefore a disagreement between experimental masses and cosine fits is observed after the first 8-10 excited levels. It indicates the need for additionnal interactions to the very simple model used, or eventually the use of different (smaller) periods.

Table VIII shows the mass parameters not given in previous tables, and the corresponding width parameters

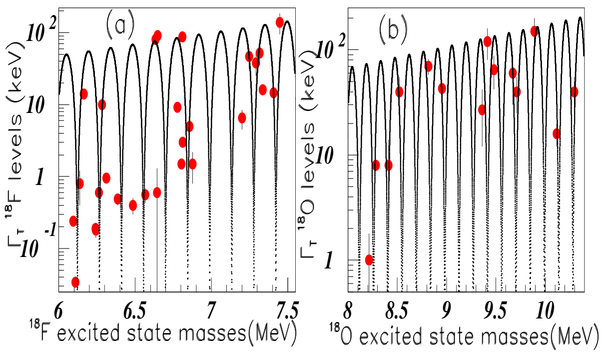

FIG. 26. Color on line. Width variation of ^{18}F (insert a) and ^{18}O (insert (b) excited levels, fitted with P = 0.145 MeV. (See text).

TABLE VII. Quantitative information concerning the oscillation behaviour of the level widths of several nuclei.

nuclei	fig.	α	β	P(keV)
^{7}Li	25a)	35	0.435	2.702
^{8}Li	24(a)	225	0.321	2.011
^{8}Be	23(a)	965	0.055	4.40
^{9}Be	24(b)	965	-0.04	2.011
^{10}Be	22(d)	5.8	0.31	2.01
^{10}B	25(b)	113	0.141	1.257
^{11}B	22(a)	5.55	0.31	1.005
^{12}C	22(b)	8750	-0.17	1.690
^{13}N	23(b)	11.0	0.42	1.29
^{13}C	23(c)	0.507	0	1.13
^{14}N	22(c)	0.19	0.6	0.408
^{15}O	23(d)	10^{-6}	2.08	0.691
^{15}N	25(c)	4.95	0.184	0.942
^{16}N	24(c)	255	-0.055	0.848
^{16}O	24(d)	24	0.22	0.942
^{17}O	25(d)	213623	-0.22	0.942
^{18}F	26(a)	5.9	0.73	0.145
^{18}O	26(b)	0.78	0.47	0.145

in order to compare the mass oscillation periods with the widths oscillation periods.

The results have been assembled by several separated ranges of mass number, leading to different oscillating periods PP. Finally all periods PP have been considered simultaneously, giving rise to a general period PPP. The PPP variation is shown in fig. 29 exhibiting a corresponding period PPP= 100.5 A.

We observe the following properties:

- in the intermediate mass range, the mass periods of oscillation for even-even nuclei, are larger than the periods of oscillation for even-odd nuclei (see figs. 14);
- the mass periods of oscillation of odd-odd nuclei, are larger than the mass periods of oscillation of odd-even

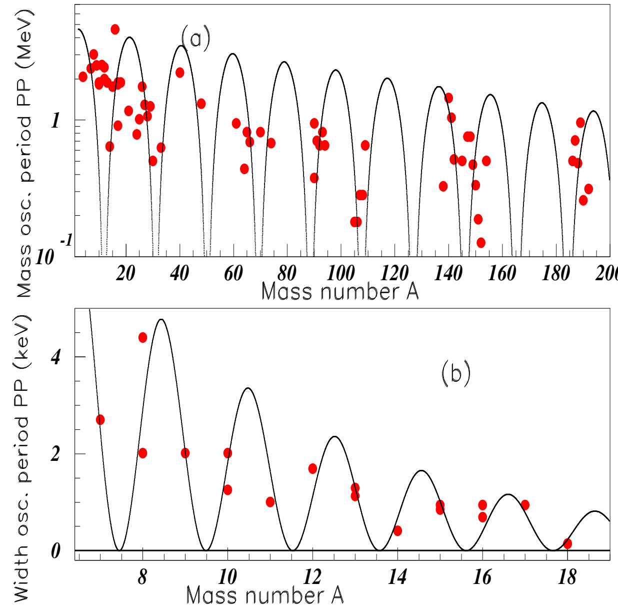

FIG. 27. Color on line. Variation of the mass oscillatory periods (insert (a)) and width oscillatory periods (insert(b) of several nuclei. (See text).

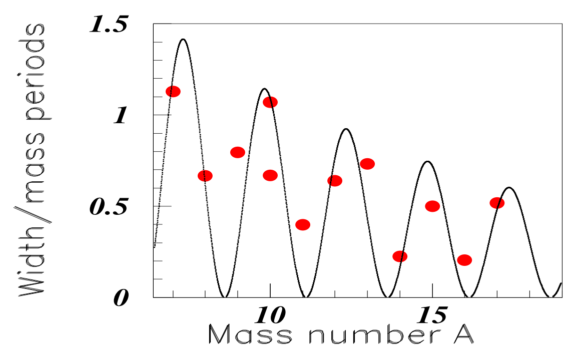

FIG. 28. Color on line. Variation of the ratio of width over mass oscillatory periods of several nuclei. (See text).

nuclei.

The mass and width oscillatory amplitudes decrease with increasing level masses. The oscillatory periods oscillate when plotted versus the nuclei mass number A. When looking the mass oscillatory periods in a restricted mass range, that is to say the variation of isotope periods, we often observe an increase of periods with the increase of neutron number. This is the case for Nitrogen and Palladium nuclei. It is not observed for period variations for a constant A (see A=17 in Table VIII).

It was shown previously in fig. 18 of [4] that an unique distribution describe, using the function (1), the masses of the following "data" :

- solar and Trappist exoplanet masses (in units of 10^{24} kg), after an homothetic factor for the exoplanet masses,

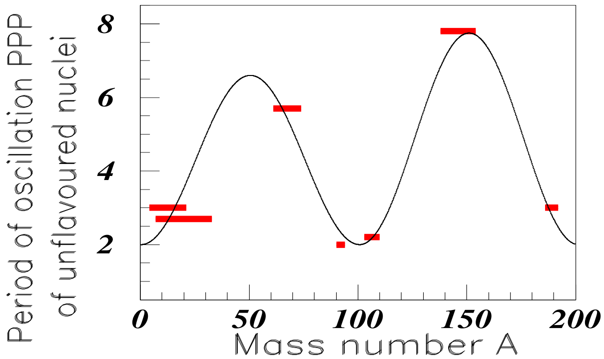

FIG. 29. Color on line. Variation of unflavoured nuclei mass periods of oscillation: PP, extracted from "data" arbitrary regrouped previously in different ranges (See text).

- quark masses (in MeV),
- lepton masses (in MeV).

It was also shown in fig.19 of [4] that an unique distribution fits the masses of the following bodies. This fig.19 of [4] is reproduced here in fig. 30. The data used inside fig.30 are:
- f2 mesons (full blue squares),
- f0 mesons (full green stars),
- Ξ baryons (full red circles) with an homothetic factor, that is to say that all masses of this family are multiply by the same factor hf=0.94,
- Ξ_C baryons, (full upside purple triangles) with an homothetic factor hf=0.91,
- ^{14}N excited state levels (black empty stars inside empty squares) with an homothetic factor hf=114.

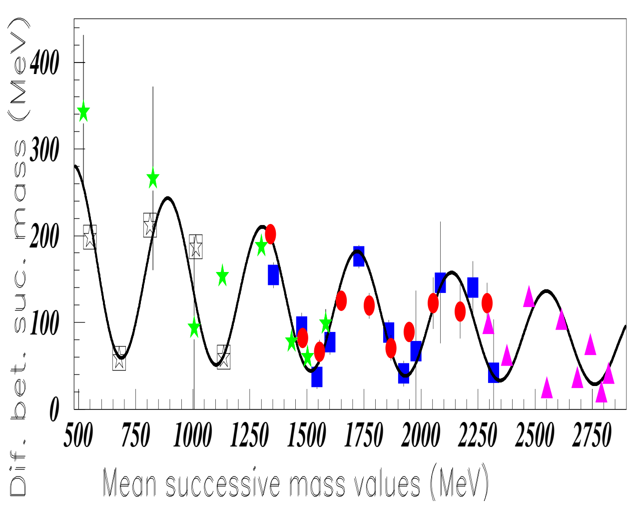

FIG. 30. Color on line. (See text). Comparison of "mass data" between several families. (see text).

Another attempt to observe the same distribution between different body's periods versus the atomic number A, is shown in fig. 31. Fig. 31 shows with full red circles, the oscillation periods of nuclear energy level masses up to A=80. Some data, encercled by black circles correspond to doubly magic nuclei. They are larger than the other red markers, but agree very well with the fit obtained with P=13.2 A. This is not the case for all other full red circle data. The blue stars correspond to the periods of the atomic energy levels of several neutral atoms [25] in units of cm^{-1} normalized by the homothetic factor 5.442*10^{-4} in order to take place in the same fig., and translated by 3A. These oscillations have been discussed in fig. 11 of ref. [2] and the corresponding data shown in Table 8 of ref.[2]. The green full squares show the periods (in keV) of hypernuclei masses [19] [20] [21] [22] discussed in [23]. We observe that the same period

TABLE VIII. Quantitative informations concerning the oscillation behaviour of nuclei analysed previously. The fig. numbers for masses are f(m) and for the widths f(Γ). The mass data parameters are notted by (m) and the width by (Γ). α(m) and P(m) are in MeV, β(m) in MeV^{-1}. The units for $\alpha(\Gamma)$ are keV, for $\beta(\Gamma)$ MeV^{-1}, and P(Γ) units are MeV.

name	f(m)	α(m)	β(m)	P(m)	f(Γ)	$\alpha(\Gamma)$	$\beta(\Gamma)$	P(Γ)
^{4}He	1(a)	0.75	0	2.07				
^{7}Li	3(a)	3.55	-0.14	2.39	25(a)	35	0.435	2.702
^{8}Li	3(b)	0.61	0.13	3.02	24(a)	225	0.321	2.011
^{9}Be	3(c)	0.84	0.072	2.51	24(b)	965	-0.04	2.011
^{10}B	3(d)	0.86	-0.03	1.88	25(b)	113	0.141	1.257
^{10}Be	4(d)	2.74	-0.12	1.88	22(d)	5.8	0.31	2.01
^{11}B	4(a)	2.4	-0.18	2.52	22(a)	5.55	0.31	1.005
^{12}B	6(d)	0.625	0	1.76				
^{12}C	4(b)	3.4	60.13	2.641	22(b)	8750	-0.17	1.69
^{13}N	5(a)	2.0	-0.13	1.76	23(b)	11.0	0.42	1.29
^{14}N	4(c)	1.65	-0.13	1.82	22(c)	0.19	0.6	0.408
^{15}N	5(b)	4.9	-0.27	1.885	25(c)	4.95	0.184	0.942
^{16}O	1(b)	19	-0.35	4.6	24(d)	24	0.22	0.942
^{17}O	6(b)	7.5	-0.45	1.82	25(d)	13623	-0.22	0.942
^{17}F	6(c)	2.7	-0.40	2.43				
^{17}N	6(a)	0.7	-0.125	1.885				
^{18}Ne	5(c)	1.5	-0.15	1.17				
^{21}Ne	5(d)	1.2	-0.255	0.911				
^{23}Mg	8	1.3	-0.3	0.333				
^{24}Mg	10(a)	3.9	-0.31	1.016				
^{25}Mg	10(b)	0.32	-0.2	0.503				
^{26}Mg	9(a)	1.25	-0.3	1.288				
^{27}Al	9(b)	0.52	-0.13	1.068				
^{28}Si	9(c)	6.3	-0.4	1.257				
^{29}Si	9(d)	0.9	-0.2	0.785				
^{30}P	10(c)	0.375	0	0.628				
^{33}S	10(d)	0.65	0	0.942				
^{33}Cl	10(d)	0.65	0	0.942				
^{40}Ca	1(c)	7.5	-0.57	2.23				
^{48}Ti	1(d)	2.1	-0.58	1.32				
^{208}Pb	1(e)	5.0	-0.81	2.07				

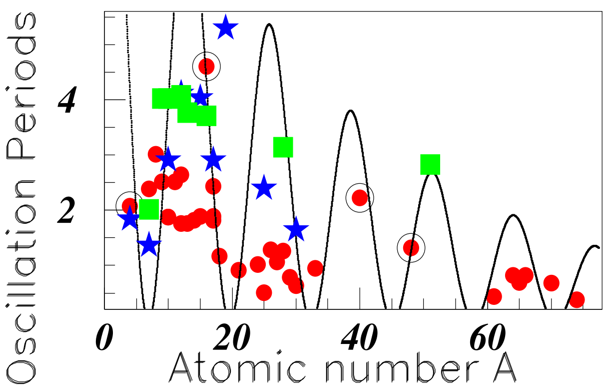

FIG. 31. Color on line. Nuclear level Periods of nuclei for A lower than ^{74}Ge nuclei compared with the periods of neutral atomic energy levels, and with hypernuclei periods. (See text).

of oscillation is able to describe the neutral atom data, the oscillation periods of the nuclear excited states, and the hypernuclear mass periods of oscillation.

V. CONCLUSION

The oscillating property of nuclei excited state masses was highlighted, as expected since the nuclei consisted of several nucleons. This corresponds to a new symmetry property, namely the symmetry of oscillation. The observation of these experimental oscillations is the main contribution of the present work.

Very good fits are observed for some nuclei mass data, for example figs. 1(a), 3(a), 3(b), ...). The fits spoil progressively for increasing level masses for increasing mass nuclei. The oscillations are unquestionable in most cases; they have been introduced consequently in those data where they are less obvious.

A damage between experimental masses and cosine fits is observed after the first 8-10 excited level masses. It indicates the need to extend the fit with introduction of smaller periods. The oscillatory amplitudes decrease with increasing level masses, with a slope increasing with the nuclei masses.

This oscillatory property allows to tentatively predict some level masses still not observed. When this may not be useful for stable nuclei since the mass of many excited states is known, this is not the case for many unstable nuclei.

The present work highlights the oscillations of nuclei level masses and widths. It does not study the oscillation amplitudes. Indeed, such study involves the need for a theoretical work, which is clearly outside the scope of this paper.

It is possible that the oscillatory behaviour will be rather generally present in nature. So it was recently observed that the Newton's gravitational constant is oscillatory as a function of time, with a period P=5.9±0.062 yr [24] [26]. In the same way, the possibility of random gaussian fluctuations of the Planck constant $\hbar$ was considered recently [27].

[1] B. Tatischeff, "Oscillation symmetry applied to: 1) hadronic and nuclei masses and widths 2) astrophysics. And used to predict unknown data.", Proceedings of the 15th International Conference on Nuclear Reaction Mechanisms, Varenna (Italy), p. 35 (2018).
[2] B. Tatischeff, "Application of the Oscillation Symmetry to the Electromagnetic Interactions of Some Particles, Nuclei, and Atoms", Journal of Advances in Applied Mathematics, Vol. 6, N. 2, 2021. doi.org/10.22606/jaam.2021.62003.
[3] B. Tatischeff, "Oscillation symmetry applied to several astrophysical data. Attempt to predict some properties of the putative ninth and tenth new solar planets", Phys. Astron. Int. J. 2019;3(6):267-274. DOI:10.15406/paij.2019.03.00193.
[4] B. Tatischeff, "Oscillation symmetry applied to several astrophysical masses, and allowing to highlight remarkable relations between masses", Phys. Astron. Int. J. 2020;4(62):93-105. DOI:10.15406/paij.2020.04.00206.
[5] C.M. Lederer, J.M. Hollander, and I. Perlman, 'Table of Isotopes Sixth Edition', John Wiley & Sons, INC., 1 (2011).
[6] D.R. Tilley, H.R. Weller, and G.M.Hale, 'Energy Levels of Light Nuclei A = 4', Nucl. Phys. A541 1 (1992).
[7] D.R. Tilley, H.R. Weller, and C.M. Cheves, 'Energy Levels of Light Nuclei A = 16', Nucl. Phys. A564 1 (1993).
[8] F. Ajzenberg-Selove, 'Energy Levels of Light Nuclei A = 16-17' Nuclear Physics **A460**1 (1986).
[9] M.J. Martin, 'Nuclear Data Sheets for A = 208', Nuclear Data Sheets 108 1583 (2007).
[10] D.R. Tilley *et al.*, 'Energy levels of light nuclei A = 8, 9, 10', Nuclear Physics A 745 155 (2004).
[11] A. Ajzenberg-Selove, 'Energy levels of light nuclei A = 5-10 ', Nucl. Phys. A320, 1 (1979).
[12] F. Ajzenberg-Selove and T. Lauristen, 'Energy levels of light nuclei (VII). A = 11-12', Nucl. Phys. A114, 1 (1968).
[13] F. Ajzenberg-Selove, 'Energy Levels of Light Nuclei A = 13-15, 'Nucl. Phys. A268, 1 (1976).
[14] D.R. Tilley, H.R. Weller, C.M. Cheves, R.M. Chasteler, 'Energy Levels of Light Nuclei A = 18', Nucl. Phys. A595 (1995) 1.
[15] D.R. Tilley, H.R. Weller, and C.M. Cheves, 'Energy levels of Light Nuclei A = 17" Revised Manuscript 2014, http://www.tunl.duke.edu/nucldata/ourpubs/17 − 1993.pdf.
[16] V. Guimarães *et al.*, 'Spectroscopic investigation of the unbound states in ^{23}Mg relevant for the ^{22}Na(p,γ)^{23} Mg reaction in novae and supernovae', proposal for Orsay PAC.pdf 2015.
[17] Y.P. Antoufiev *et al.*, 'Energy levels of the ^{28}Si nucleus', Nucl. Phys. **54** 301 (1964).
[18] G. Brown *et al.*, 'Level positions of some Cu, Zn, Ga, and

Ge isotopes', Nucl. Phys. A**101** 163 (1967).

[19] H. Hotchi *et al.*, 'Spectroscopy of medium-heavy Λ hypernuclei via the (π^+, K^+) reaction ', Phys. Rev. C 64, 044302 (2001).

[20] O. Hashimoto and H. Tamura, 'Spectroscopy of Λ hypernuclei', Progress in Part. and Nucl. Physics 57, 564 (2006).

[21] T. Gogami *et al.*, 'High resolution spectroscopic study of ${}^{10}_{\Lambda}$Be', Phys. Rev. C 93, 034314 (2016).

[22] D.J. Millener, 'Hypernuclear structure from γ-ray spectroscopy', arXiv:nucl-th/0402091v1 (2004).

[23] B. Tatischeff, "Connections between Hadronic Masses in the one Hand and between Fundamental Particle Masses in the other Hand", Journal of Advances in Applied Mathematics, 53, 104 (2020). DOI:10.22606/jaam.2020.53002.

[24] J.D. Anderson, G. Schubert, V. Trimble, and M.R. Feldman, 'Measurements of Newton's gravitational constant and the length of day', Europhys. Lett. **110**, 10002 (2015).

[25] https://physics.nist.gov/PhysRefData/HandbookTales /"atom"table5.htm.

[26] S. Schlamminger, J.H. Gundlach, and T.D. Newman, 'Recent measurements of the gravitational constant as a function of time', Phys. Rev. D **91**, 121101(R) (2015).

[27] G. Mangano, F. Lizzi, and A. Porzio, 'Inconstant Planck's constant', arXiv:1509.02107v1 [quant-ph] (2015).